

TESTING RESULTS OF MAJOR COMPONENTS AND PROGRESS REPORT OF TLS SUPERCONDUCTING CAVITY PROJECT

G.H. Luo, L.H. Chang, C.T. Chen, F.Z. Hsiao, C.C. Kuo, M.C. Lin, Ch. Wang, T.T. Yang, M.S. Yeh, and M. Pekeler⁺
 Synchrotron Radiation Research Center, Hsinchu 300, Taiwan, R.O.C.
⁺ACCEL Instruments GmbH, 51429, Bergisch Gladbach, German

Abstract

The superconducting 500 MHz cavity of CESR-III design has been chosen to replace the existing room temperature copper cavities. A turbine type cryogenic plant will provide adequate cooling capacity, 450 W, for the operation of the SRF cavity and superconducting multipoles wiggler at 4.5 K. The installation of SRF cavity and cryogenic system is scheduled during late 2002. Commissioning of the SRF cavity, cryogenic system and the superconducting multipoles wiggler is planned in the early 2003. The overall status of this project and some testing results of major components of SRF cryostat will be presented.

1 INTRODUCTION

The Taiwan Light Source (TLS) provides 200 mA, 1.5 GeV electron beam to generate photon source for academic and industrial research scientists. The storage ring is a six-fold symmetry Triple-Bend-Archomat (TBA) lattice with six straight sections. Four of the straight sections are occupied by conventional normal-conducting insertion-devices, U9, U5, W20 and Elliptical Polarized Undulator EPU5.6. One straight section is used as injection taken by 4 kickers. A 3-poles and 6.5 Tesla superconducting wavelength shifter was installed at downstream of the injection kicker #3 to provide high photon flux in x-ray regime. One RF straight section is for the Doris cavities and diagnostics instrumentation, e.g. current transform and excitation kicker for transverse feedback. The renovation plan of 2003 will install one SRF cryomodule and one 29-poles' 3.5 Tesla superconducting multipoles-wiggler in the RF straight section.

There are three operational Doris cavities installed to provide electrons acceleration and energy compensation at TLS's booster and storage ring. One Doris cavity functions and operates as expected in the booster ring to provide beam acceleration with great reliability. However, the double cavity set with damping antenna attached to each cavity port did not provide sufficient damping mechanism for the excited Higher Order Modes (HOMs) at storage ring. A plunger-type tuner with precision controlled cavity body temperature has been implemented for each cavity. These efforts with RF voltage modulation keep the stability of photon spectrum within acceptable range for general synchrotron users.

It has been a strong demand to increase the photon flux by at least a factor of two with the same lifetime and

better photon stability from users' community. Evaluation of a third Doris cavity, PEP-II cavities, or a SC cavity was carried out during 1998. The potential of operating SRF cavity up to 8 MV/m with 200 kW is very attractive to TLS. The SC cavity extends large flexibility for tuning the cavity to optimize the operation parameters.

The CESR's SC cavity, as shown in Fig. 1, has been selected and contracted to ACCEL for manufacturing on March 2000. The large beam duct on both side of the cavity will help the HOM being coupling out of the cavity without reducing the Q-value of the fundamental modes. A comparison of operation parameters for Doris cavity and CESR's SRF cavity is shown in Table 1.

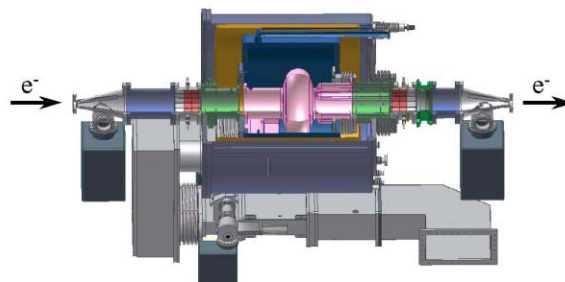


Figure 1. Profile of SRF cavity to be installed at TLS

Table 1 . The comparison of operating parameters for the Doris cavities and SRF cavity.

Parameter	Doris cavity	SRF cavity
Beam Energy (GeV)	1.5	1.5
Circumference (m)	120	120
RF Frequency (MHz)	499.666	499.666
Harmonic Number	200	200
Beam Current (mA)	200	500
Energy Spread	0.075%	0.075%
Bunch Length (mm)	9.2	6.5
Compaction Factor	0.00678	0.00678
Energy Loss (keV/turn)	128	128 (168)
RF Gap voltage (kV)	800	1600
Number of Cavities	2	1
Number of klystrons	2	1
Wall Dissip. (W/cavity)	27.5k	<30
Beam Power (kW)	64	64 (84)
Klystron P _{out} (kW/kly.)	60	60 (100)
R _s /Q ₀	77.441	44.5
Synchro. Freq. (kHz)	26.5	37.8
Energy Acceptance	± 1.4%	± 2.1%
RF Transmission Line	EIA6 1/8"	WR1800
Tuning Angle Offset	0°	0° > ψ _{offset} > 10°

2 MAGNETIC SHIELDING SIMULATION AND MESUREMENT

The superconducting RF cavity is very low in surface resistance, which makes the cavity can have very high accelerating gradient but very low power dissipation on the cavity wall. However, surface resistance of superconducting cavity can be deteriorated by various sources. According to BCS theory, one of the major sources is the trapped DC magnetic field for type II material, e.g. Nb. The magnetic shielding for pure Nb cavity will be the major parameter that affects the performance of the cavity and also the cryogenic loss.

A HOM damped SRF cavity is normally designed with large beam pipe to couple out the HOMs and using the absorbing material to absorb the HOMs' power at room temperature. A large beam tubes make the magnetic shielding difficult due to the big holes at both ends of the cavity.

For a uniform magnetic field and perpendicular to the cavity axis, the attenuation factor of shielding can be estimated by analytic theory [1]. For a field parallel to the cavity axis, the analytic solution cannot provide a reasonable estimation of the attenuation factor for a finite cryostat length with large opening at both end caps.

A 3-D finite element solver, TOSCA [2], has been used to find the attenuation factor at the center of Nb cavity. The 3-D model of SRF cryostat is constructed according to the engineering structure. The attenuation factors of original cryostat, which is shielded by one layer's ADMU-80 in room temperature and one layer in LN₂ temperature, under different external field are simulated as shown in Fig.2 with solid dot. From data sheet, permeability of ADMU-80, at LN₂ temperature, will reduce to only 10% of that in the room temperature. This significantly reduces the attenuation factor.

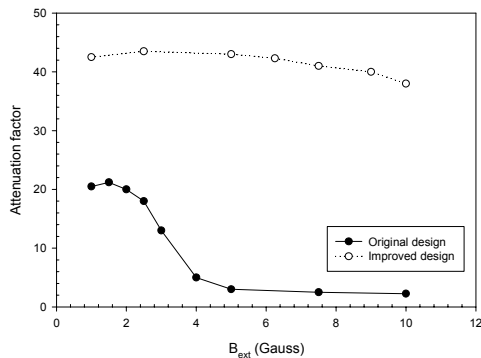


Figure 2. Attenuation factor of external magnetic field for original design and new design with varies field strength.

For a modified shielding design, a cryoperm is used in the cryostat at LN₂ layer and the thickness of ADMU-80, at room temperature, increased to 1mm. The overall

attenuation factor of new shielding design increases by a factor of two and extends to higher external field, as shown in Fig.2. The measured attenuation factor is better than 50 at earth field.

3 NIOBIUM CAVITIES, RF WINDOWS AND CRYOGENIC SYSTEM

The Nb cavity is manufactured by ACCEL through E-beam welding and pressurized with Argon for shipment to Cornell University. The vertical test results are shown in Fig. 3 under LHe temperature of 4.2 K. The black dots indicated the first measurement after the multipacting processing. The red dots were recorded after the helium processing. From the diagram, Fig. 3, we can find the Q₀ is 1.4*10⁹ at 7 MV/m, which is much better than the specified gradient 5.33 MV/m.

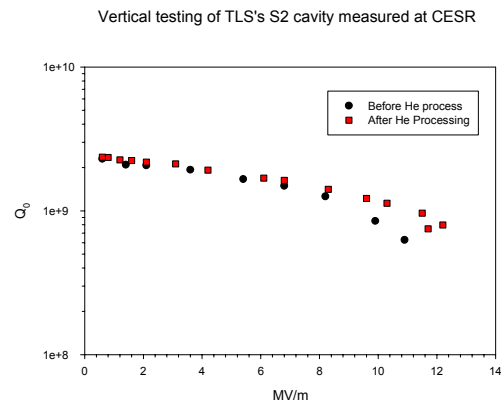


Figure 3. The Q₀ verse the acceleration gradient before and after He processing.

A long-period baking of the RF windows and other waveguide components were requested prior to assemble with SRF module in order to reduce outgas from waveguide system. In addition to baking, RF window will be high power processing up to 200 kW CW in traveling wave mode and 50 kW CW in standing wave mode with various phases. These approaches will be very helpful to minimize the in-situ processing time and to reduce outgas from ceramic window. The coating of TiN is in the thickness of 30-50 Å to avoid the multipacting on the window. The different slopes of thermal gradient for two windows are mainly contributed to the difference of purity control of ceramic [3]. Thickness of TiN coating contributes minute to the heat loss of RF window. The temperature gradient is measured by IR camera during the RF processing. Figure 4 shows the summary of temperature gradient of two windows under different processing power and processing modes. The two dots at power level of 256 kW represent the case of standing wave processing. The phase did not set to a position such that peak amplitude of standing wave reached maximum value at the windows.

4 SUMMARY

The RF structure and cavity models were setup to simulate the RF properties by HFSS [4] and ANSYS [5,6]. A 3-D cryostat model for the analysis of magnetic shielding has completed by TOSCA. A new magnetic-field shielding design was implemented in the cryostat. A quasi-asymptotic analysis has accomplished [7] accordingly. The Nb cavities' vertical testing, HOM dampers and RF windows processing were tested and performed at CESR with satisfactory results. A prototype direct feedback system has been test with Doris cavities to combat heavy beam loading effect. The safety evaluation of cryostat has completed and presented to TLS Safety Committee. A turbine type cryogenic system with 450 W capacities at 4.5 K was contracted to Air-Liquide. Major sub-components of cryogenic system were tested. One of the SRF cryomodule will ship to SRRC before the end of this year for acceptance test. Beam commissioning will be carried out during the second quarter of 2003.

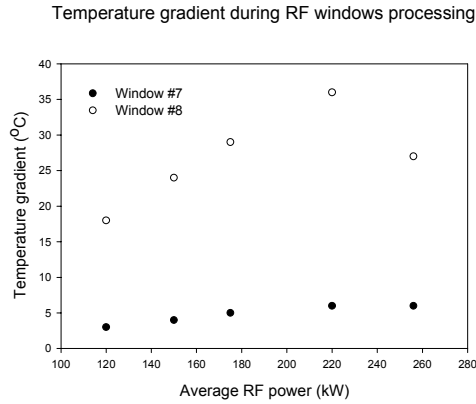


Figure 4. Summary of temperature gradient verse processing power for two RF windows in CW and standing wave modes.

The cryogenic plant is a turn-key system, which is contracted to Air Liquide. The major components of the 4.5K cryogenic plant include two screw compressors, two oil removals, one refrigerator/liquefier with turbine-type expander, two warm gaseous helium storage tanks with the size of 100 m³ each, one main liquid helium dewar with full capacity of 2000 liters, and one recovery compressor. The cryogenic plant shall be able to provide a minimum 110 liters/hour of liquification capacity and 450 W refrigerating capacities at 4.5 K with pre-cooling of cold box by LN₂. A frequency driver is used to regulator the output efficiency of screw compressor to conserve the operation cost

Estimation of the cryogenic capacity is based on the operation experience of CESR-III cryomodule and the available data sheet for commercial products. A 50% of engineering safety factor is added to the estimated cryogenic loss. A 3-dimensional schematic layout of new utility building, compressor room, the cryogenic piping, the platform for refrigerator and high-power RF feed line is shown in Fig. 5.

5 ACKNOWLEDGEMENT

The authors are especially appreciated to H.Padamsee, S. Belomestnykh, J. Knobloch, R.J. Geng, J. Sears, P. Quigley, J. Reilly, R. Enrllich, M. Tigner and staffs at LNS laboratory, Cornell University, in setting up the testing system and constant guidance during our visiting. The HFSS simulation program is supported by National Center for High-performance Computing (NCHC) in Taiwan.

6 REFERENCES

- [1] A. Mager, J. Appl. Phys., p.1914, 1968
- [2] TOSCA, Vector Fields Limited, England, 1994.
- [3] B. Dewager, SRF workshop 2001, Tsukuba, Japan, to be published.
- [4] HFSS, by Ansoft Corp., Pittsburgh, 1999.
- [5] ANSYS, by ANSYS Inc., Canonsburg, PA, 1994.
- [6] M.C. Lin et. al., p.1207, PAC'01, Chicago, USA.
- [7] L.H. Chang et. al., ISPM, 2001, to be published.

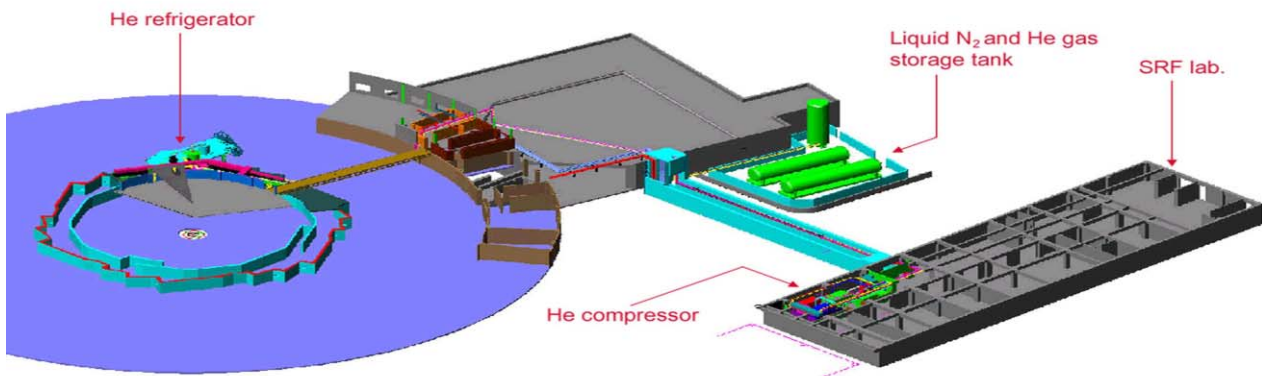


Figure 5. Schematic layout of compressor room, SRF lab, cryogenic piping, and platform for refrigerator